Technological process modeling for ink filling in the high accuracy screen printer mesh

H A Hilal, S N Litunov, S V Belkova, S S Bochkareva and E N Trifonova
Omsk State Technical University, 11 Mira ave., 644050, Omsk, Russia

E-mail: litunov-sergeyy@rambler.ru

Abstract. Printed electronics is a modern direction in developing technology of electronic components production. The purpose of the work is to control the thickness of the conductive pattern on the print obtained by screen printing. The task of the study is to develop a mathematical model for ink filling the screen mesh. The calculations took the speed of the dosing squeegee of 2...20 cm/s, inclination angles of 75°...105°. The design pressure is in the range of 2082.08...34604.2 PA, the estimated depth of ink filling the mesh is 25...280 microns.

1. Introduction

The development of electronics production has led to the emergence of new technologies to produce components of printed electronics. Screen printing method plays an important role allowing one to form a layer of conductive material with the required thickness on the substrate. Analysis of technical information shows the growth of the screen printing use in the field of printed electronics [1-11]. However, the weakness of screen printing is the mesh deformation of the printed form, resulting in a decrease in the density of installation and accuracy of electronic components. To improve the accuracy of the reproduced image, a device with a dosing and cylindrical squeegee is proposed [12]. The use of such a device allows one to dose accurately the ink in the mesh. Schematic layout of the screen printing device is shown in figure 1.

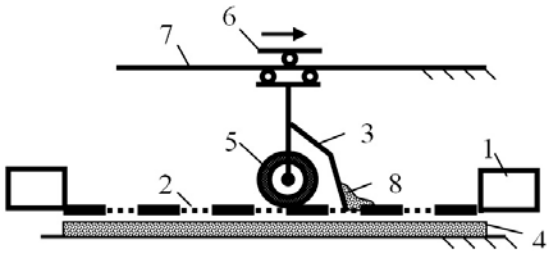

Figure 1. Figure 1. High-precision screen printing device:
1 – shaped frame; 2 – plate; 3 – dosing squeegee; 4 – substrate; 5 – cylindrical squeegee; 6 – carriage; 7 – guides; 8 – ink.

The dosing squeegee in the form of a thin plate must form such a pressure that the ink does not go beyond the mesh from the substrate. The movement velocity and the dosing squeegee inclination angle at a constant ink viscosity influence the hydrodynamic pressure. The paper shows the development of a technological process model of filling the mesh with ink under the pressure arising during the movement of the plate on a flat surface.

Content from this work may be used under the terms of the Creative Commons Attribution 3.0 licence. Any further distribution of this work must maintain attribution to the author(s) and the title of the work, journal citation and DOI.
Published under licence by IOP Publishing Ltd

The ink moves in front of the dosing squeegee in the form of a rotating roller, the length of which exceeds its transverse dimensions. On this basis, consider a flat, two-dimensional flow. The ink flow is shown schematically in figure 2.

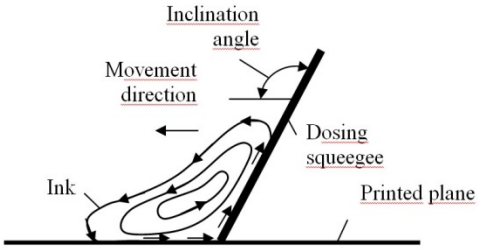

Figure 2. Ink movement in front of the dosing squeegee.

On moving the dosing squeegee, a hydrodynamic pressure is formed, under which the ink fills the meshes of the printed plate. To develop the model, we apply the scheme of flow around a plate of infinite length and located across the flow.

2. Theory

The development of electronics production has led to the emergence of new technologies to produce components of printed electronics. Screen printing method plays an important role allowing one to
According to Prandtl hypothesis, at a short distance from the impermeable boundary of the flow, which is called the boundary layer, the liquid velocity increases sharply and becomes equal to the total flow one. Outside the boundary layer, the viscous liquid flow does not differ from the ideal liquid one. This makes it possible to use the model of inviscid liquid motion to develop the model.
Assume that:

- the ink volume in front of the dosing squeegee is constant;
- the ink movement is stationary;
- ink is incompressible;
- the dosing squeegee is absolutely rigid.

In the absence of external forces, the motion of the inviscid liquid is described by Euler and continuity equations:

$$\begin{cases} \dfrac{\mathrm{d}V}{\mathrm{d}t} + \left(\bar{V}, \nabla\right)\bar{V} = -\dfrac{1}{\rho}\operatorname{grad} P + \bar{F} \\ \operatorname{div}\bar{V} = 0, \end{cases}$$

where V is the velocity, P is the pressure, ρ is the liquid density, F is mass forces.
There are scalar functions: $\varphi(x,y)$, called the velocity potential, and $\psi(x,y)$, called the stream function, such that:

$$\frac{\mathrm{d}\varphi}{\mathrm{d}x} = u, \quad \frac{\mathrm{d}\varphi}{\mathrm{d}y} = v,$$

$$u = \frac{\mathrm{d}\psi}{\mathrm{d}y}, v = -\frac{\mathrm{d}\psi}{\mathrm{d}x}.$$

where u, v are projections of the velocity vector on the axis *OX*, *OY*, respectively.
The set of functions φ and ψ is an analytical function $w(z)$ and called a complex potential of the flow:

$$w(z) = \varphi(x, y) + i\psi(x, y)$$

One can determine the flow rate from the expression

$$\frac{\mathrm{d}w}{\mathrm{d}z} = \bar{V}(z) = u - \mathrm{i}v,$$

where $\bar{V}(z)$ is the complex velocity that is coupled to the real velocity with respect to the *OX* axis.

The pressure was determined by Bernoulli integral:

$$\frac{V^2}{2}+\frac{P}{\rho}-U=A, \tag{1}$$

where U is the potential of mass forces, $V=\left(u^2+v^2\right)^{1/2}$, A = *const*, ρ is the liquid density; u, v are projections of the velocity vector on the coordinate axis.

In the given barotropic potential motion of an ideal incompressible homogeneous liquid, the value A is constant at any point of the liquid mass. Assuming that at infinity the flow borders the atmosphere, take A equal to atmospheric pressure. The mass force potential in question is the static pressure of the liquid at the point under consideration, that is, U=gZ, where g is the gravity force; Z is the height of the liquid column above the point under study. The height of the ink layer in front of the dosing squeegee does not exceed 1 cm, the proportion of printed screen inks is up to 1.5 g/cm^3, and paste with metal particles is 4.8 g/cm^3. Under these conditions, the potential of mass forces can be neglected. Expression (1) takes the form:

$$P=\left(\frac{V_\infty^2-V^2}{2}\right)\rho-P_{atm},$$

where P_{atm} is atmospheric pressure, V_∞ is flow rate at infinity.

3. Development of mathematical model

To develop a dosing squeegee flow model, we used the model of potential translational inviscid liquid flow around a pair of plates symmetrically arranged and rotated relative to the horizontal axis. The design scheme is shown in figure 3.

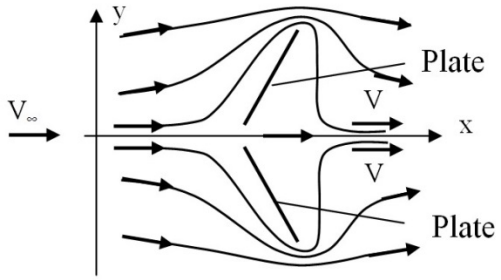

Figure 3. Inviscid liquid flow around a pair of plates.

A translational flow, having the velocity Vat infinity, rises on a couple of the plates. Since the plates are arranged symmetrically with respect to the horizontal axis, a stream line is formed during their flow, which coincides with the axis of symmetry. On this stream line, the velocity has only a horizontal component, and the vertical one is zero, so this stream line is considered an impenetrable boundary. If we consider only the upper half-plane, without the lower one, the flow is the movement of the plate, touching the lower plane end and located at an angle to it.

Flow around a homogeneous inviscid liquid flow with circulation of a thin infinite length plate perpendicular to the flow is described by the equation obtained by Joukowski transformation [13, p. 187]:

$$W(z)=\frac{1}{2}\left[\vec{V}_\infty\left(z+\sqrt{z^2-c^2}\right)+\frac{1}{2}V_\infty\left(z+\sqrt{z^2-c^2}\right)\right]+\frac{G}{2\pi}\ln\left(z+\sqrt{z^2-c^2}\right) \tag{2}$$

where V is the flow velocity at infinity; $z=x+iy$; $c^2=a^2+b^2$; a, b are the long and short ellipse radii, respectively (b = 0).

Expression (2) is a conformal map of the ellipse neighborhood to the neighborhood and the inside of the circle and simulates the flow around the plate, located horizontally at the origin, the translational flow at an angle of 45° to the plate (figure 4). But, according to figure 2, the plate should be shifted relative to the origin and rotated to the horizontal axis.

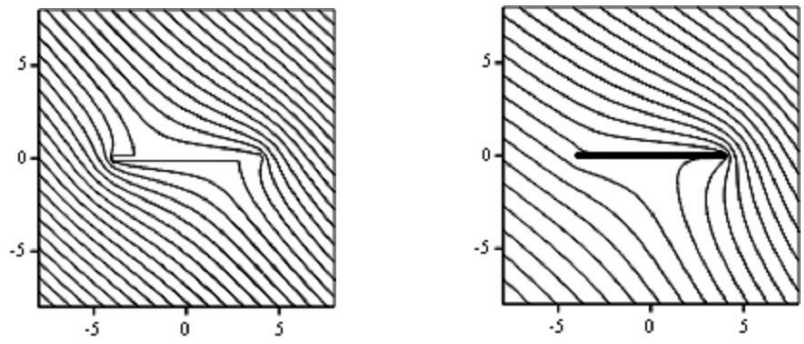

Figure 4. The pattern of translational plate flow:
$a = 3$, on the left $G = 0$, on the right $G = 2\pi a u_\infty$.

The rotation of the complex plane relative to the another one is due to the multiplication of the original plane coordinates on $e^{i\alpha}$, that is, in the rotated plane $z' = z\,\mathrm{e}^{\mathrm{i}\alpha}$. Considering that

$$z' = (x + \mathrm{i}y)(\cos\alpha + \mathrm{i}\sin\alpha),$$

where α is the rotation angle of one coordinate system relative to the original one, we have

$$W'(z) = \frac{1}{2}\left[\vec{V}_\infty\left(z' + \sqrt{z'^2 - c^2}\right) + \frac{1}{2}V_\infty\left(z' + \sqrt{z'^2 - c^2}\right)\right] + \frac{G}{2\pi}\ln\left(z' + \sqrt{z'^2 - c^2}\right), \quad (3)$$

Omitting the cumbersome but not complex transformations of expression (3), carried out using the known Euler and Moivre formulas, we obtain:

$$W' = \frac{1}{2}V_\infty\left[A(z') + B(z') + C(z')\right],$$

where,

$$A(z') = \mathrm{e}^{i\alpha}\left(z' + \sqrt{z'^2 - c^2}\right) = \left[(P\cos\alpha - Q\sin\alpha) + (Q\cos\alpha + P\sin\alpha)\right],$$

$$P_A = \left[x'' + R_A\cos\left(\frac{\beta + 2\pi k}{2}\right)\right],$$

$$Q_A = \left[y'' + R_A\sin\left(\frac{\beta + 2\pi k}{2}\right)\right],$$

$$x'' = x\cos\gamma - y\sin\gamma,\ y'' = x\sin\gamma + y\cos\gamma;$$

where k is the order of the root (for this case $n = 2$); γ the angle between the direction of the translational flow at infinity and the plate;

$$R = \left[\left(x''^2 - y''^2 - c^2\right)^2 + \left(x''y''\right)^2\right]^{1/2};$$

$$\beta = \mathrm{arctg}\left(\frac{2x''y''}{x''^2 - y''^2 - c^2}\right),$$

$$B(z') = P_B - \mathrm{i}Q_B = z' - \sqrt{z'^2 - c^2},$$

$$P_B = \left[x'' - R_A\cos\left(\frac{\beta + 2\pi k}{2}\right)\right],$$

$$Q_B = \left[y'' - R_A\sin\left(\frac{\beta + 2\pi k}{2}\right)\right],$$

$$C\left(z^{"}\right)=\frac{G}{2\pi \mathrm{i}}\ln\left(z^{"}+\sqrt{z^{"2}-c^{2}}\right)=\frac{G}{2\pi}\left(\operatorname{arctg}\frac{Q_A}{P_A}-\mathrm{i}F\right),$$

$$F=\left(P_A{}^2+Q_A{}^2\right)^{1/2}.$$

The angle of plate rotation relative to the translational flow is determined by the ratio

$$\gamma=\pi-\alpha\ .$$

Figure 5 shows the streamlines and the surface of the stream function of translational flow obtained by the conformal map according to Joukowski formula. The flow pattern is obtained using the first term of the right part (3). Streamlines are ones of equal values of the stream function obtained as lines of surface intersection of the stream function and planes parallel to the horizontal plane.

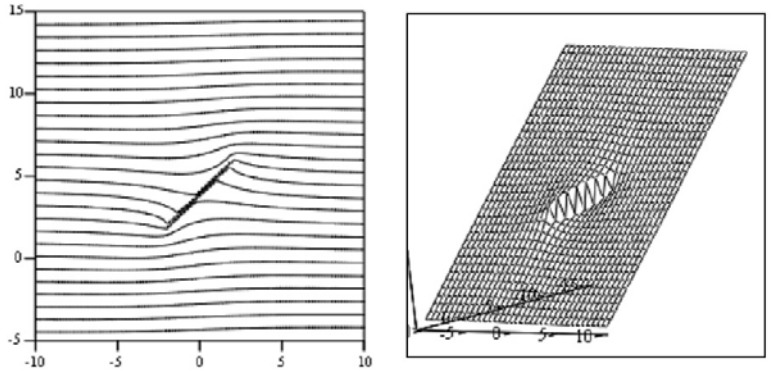

Figure 5. Streamlines (left) and stream function (right):
the plate inclination angle relative to the translational flow α = 45°; V = 1 m/s.

At z, the surface of the steam function tends to the plane. At $z = a$ on the surface a vertical elliptical incision, causing a flow perturbation, is formed. When moving away from the plate, the flow perturbation fades, which is consistent with the real flow.

To simulate the plate flow, it is necessary to place a dipole describing the second term (3) in the translational flow. Figure 6 shows the streamlines and the surface of the dipole stream function.

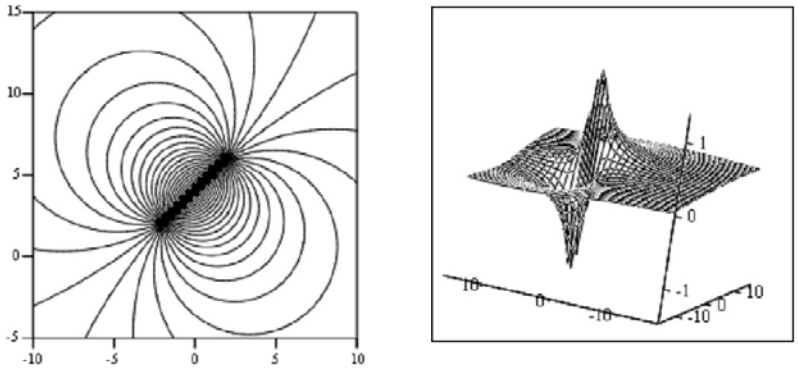

Figure 6. Streamlines (left) and stream function (right) of the dipole:
in a stationary liquid: α = 45°.

As in the previous case, at $z \to \infty$ the stream function tends to the plane. The dipole inclination angle relative to the translational flow corresponds to the plate inclination angle to the translational flow α = 45°. The dipole feature is its elongation along the segment equal to the plate length.

Figure 7 shows the image of a vortex located at an angle α = 45° with respect to the axis *OX*. The image corresponds to the third term (3). Circulation induced by the vortex filament forms a nonzero velocity at the lower end of the plate [13] $G = 2\pi a u_\infty$.

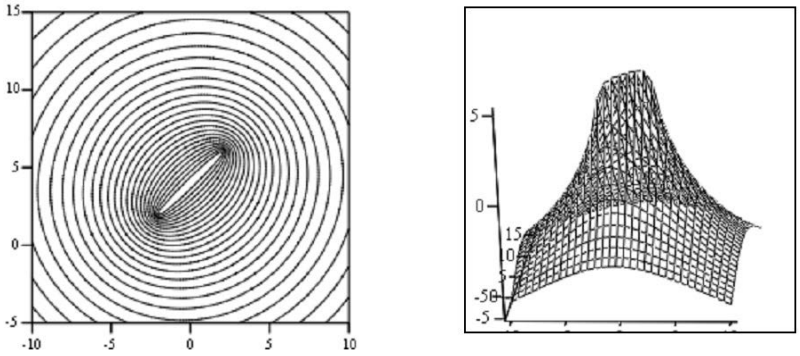

Figure 7. Streamlines (left) and stream function surface (right) of the vortex located in a stationary liquid.

Figure 8 shows the total flow, including the translational flow, dipole and vortex. The figure illustrates the direction of circulation with an arrow.

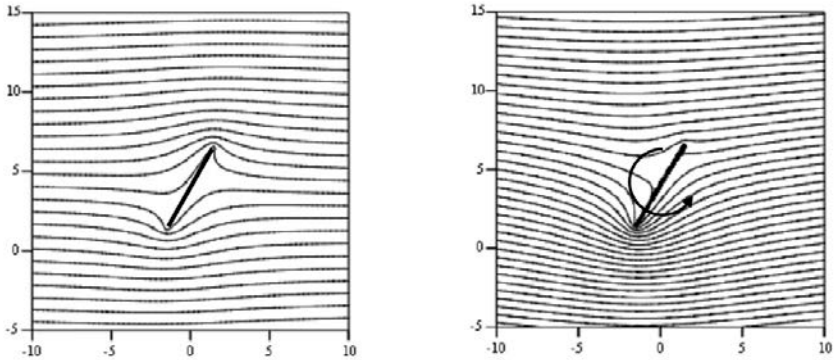

Figure 8. Translational plate flow at an angle of 45° on the left without circulation; on the right with circulation $G = 2\pi a u_\infty$.

To simulate the flow around a pair of plates arranged symmetrically with respect to the horizontal axis, we obtained an analytical continuation of the function W(z) from the upper half-plane to the lower one. To do this, we built a function $W(\bar{z})$,where $\bar{z}$ is the complex variable, conjugate of z.

After replacing a complex variable z = x + iy on $\bar{z} = x - iy$, folding the complex potentials and selecting the imaginary part from them, we received expression for the stream function $\psi(z)$ and $\psi(\bar{z})$, on which the flow pattern shown in figure 9 was built.

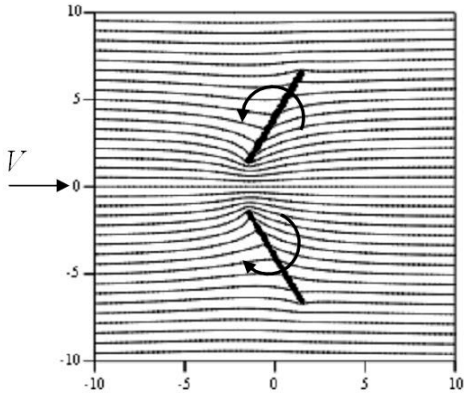

Figure 9. Translational flat-plate flow with circulation.
The arrow shows the direction of the translational flow.

The figure shows that the streamline, located on the axis of symmetry between the plates, is a straight line and simulates the plane where the plate moves. Dropping the lower half-plane, we consider the flow only at the upper one. To calculate the pressure arising under the action of the dosing squeegee, the velocity distribution on the symmetry line was determined. Taking a derivative of the stream function, we obtained expressions for velocity projections on the coordinate axis for the translational flow, dipole and vortex. In the formulas, the letter u denotes the velocity projection on the OX axis, the letter v - on the OY axis. Indices indicate the corresponding flow component:

$$u_{trans} = \frac{1}{2}V_\infty \left\{ \cos\alpha + \frac{1}{R}\left[x^{"} \cos(\alpha - \beta) + y^{"} \sin(\alpha + \beta) \right] \right\},$$

$$v_{trans} = -\frac{1}{2}V_\infty \left\{ \sin\alpha + \frac{1}{R}\left[x^{"} \sin(\alpha + \beta) + y^{"} \cos(\alpha - \beta) \right] \right\},$$

$$u_{dip} = V_\infty \left\{ 1 - \frac{1}{R}\left[x^{"} \cos(\beta) + y^{"} \sin(\beta) \right] \right\},$$

$$v_{dip} = -V_\infty \left\{ \frac{1}{R}\left[x^{"} \sin(\beta) - y^{"} \cos(\beta) \right] \right\},$$

$$u_{vort} = -\frac{G}{2\pi}\left(Re_k \cdot Im_m + Re_m \cdot Im_k \right)$$

$$v_{vort} = -\frac{G}{2\pi}\left(Re_k \cdot Re_m + Im_m \cdot Im_k \right)$$

where

$$Re_k = 1 + \frac{x^{"} \cos\beta + y^{"} \sin\beta}{R},$$

$$Im_k = -\frac{x^{"} \sin\beta + y^{"} \cos\beta}{R},$$

$$Re_m = \frac{x^{"} + R\cos\beta}{Y},$$

$$Im_m = -\frac{y^{"} + R\sin\beta}{Y},$$

$$Y = \left(x^{"} + R\cos\beta \right)^2 + \left(y^{"} + R\sin\beta \right)^2.$$

The flow rate is determined by the expression

$$V = \left[\left(u_{trans} + u_{dip} + u_{vort} \right)^2 + \left(v_{trans} + v_{dip} + v_{vort} \right)^2 \right]^{1/2}.$$

To determine the ink velocity in the mesh, the assumptions were made: the mesh is a round hole; the ink flow is stationary. Poiseuille's law was used to determine the depth of ink filling the meshes

$$V = \frac{\left(P_1 - P_2 \right) r^2}{l 4 \mu}, \tag{4}$$

where V_h is the flow rate of ink in the hole, r is the radius of the hole, equal to the circle, inscribed in a square with a side equal to the side of the mesh; P_1-P_2 is pressure drop in the mesh; μ is dynamic ink viscosity; l is the mesh height.

Preliminary experiments have shown that the ink begins moving in the mesh only when a certain pressure (called the pressure of the filtration beginning) is reached. Figure 10 represents the design scheme to determine the pressure and time of the ink flow through the mesh. The experiments showed that for mesh № 165-34 the pressure of the filtration beginning for ink with viscosity of 12 PA is 2432 PA.

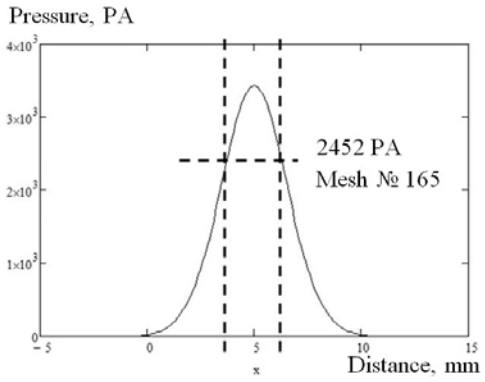

Figure 10. Example of the pressure distribution in front of the dosing squeegee:
the squeegee inclination angle of 75°;
the squeegee velocity of 20 cm/s.

The figure shows that the ink flows through the mesh during the time for which the squeegee passes 0.25 cm. At the squeegee velocity of 2 cm/s, the time during which the ink flows through the mesh is 0.125 s. Since the pressure at the outlet of the mesh is atmospheric, the pressure drop is equal to the pressure at the inlet of the mesh. For mesh №. 165-34, the radius r = 13.3 μm. The height of the mesh (mesh thickness) is 62 μm. The average flow rate of the ink in the mesh will be V = $219.2 \cdot 10^{-6}$ m/s. For 0.125 s, the liquid will pass a distance of $25.3 \cdot 10^{-6}$ m/s, that is, the mesh will be filled by 40.8 %.

4. Results and discussion

The calculated ink pressure distribution in front of the dosing squeegee is shown in figure 11.

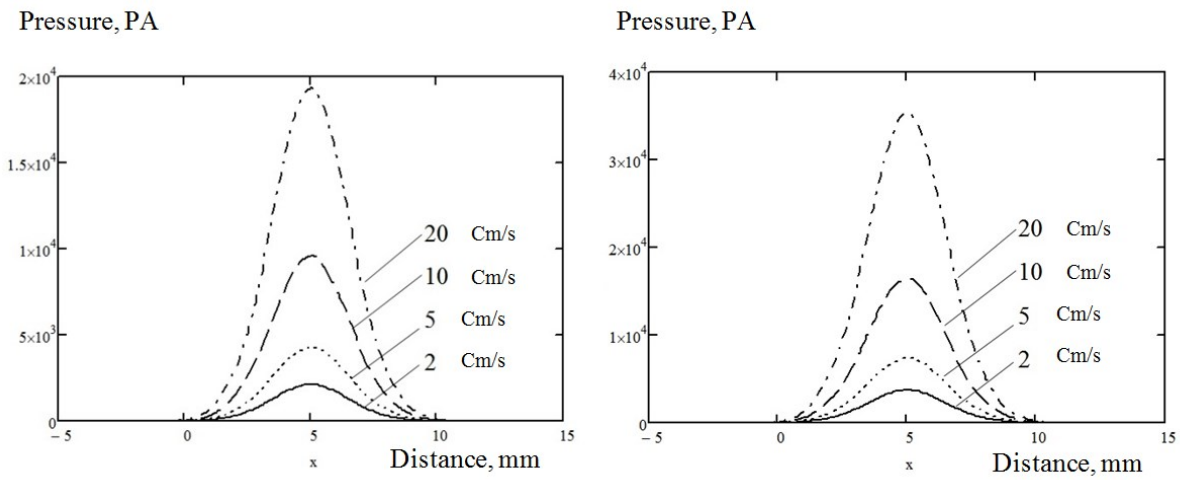

Figure 11. Liquid pressure induced by the flow motion during the plate flow, located at an angle of 75° (left) and 105° (right) from the horizontal axis.

From the figures it can be concluded that the result qualitatively coincides with the practical data, according to which the "negative" squeegee forms significantly less pressure than the "positive" one.
Figure 12 shows the dependence of the depth of the ink filling the meshes 165-34 on the dosing squeegee inclination angle and its velocity, calculated according to the equation (4). Calculations were performed for the dosing squeegee inclination angles of 75°, 80°, 100°, 105°. Dotted lines indicate the angles for which the calculations were not performed. The distance, where the ink pressure exceeds the pressure of the filtration beginning while moving the dosing squeegee, was determined by standard MS EXEL functions.

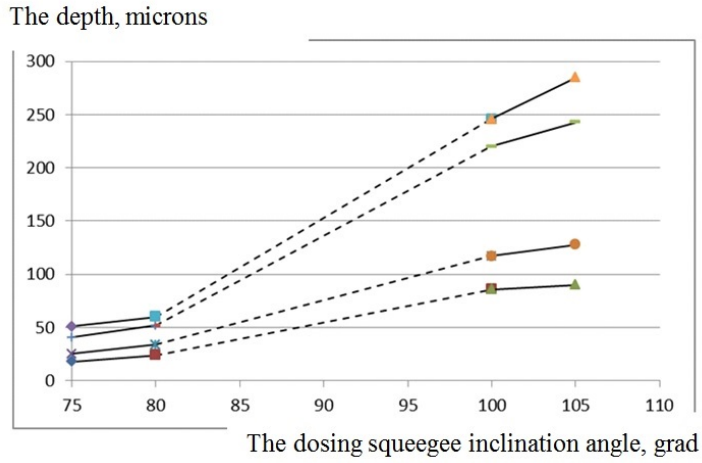

Figure 12. The depth of ink filling the meshes:
dosing squeegee velocity (bottom up) 2 cm/s, 5 cm/s,
10 cm/s, 20 cm/s.

The figure shows that the depth of the ink flow through the mesh exceeds its height at "positive" inclination angles of the dosing squeegee. Thus, at inclination angle of 105°, the depth of flow is 280 microns. Experiments have shown that with these parameters it is possible to achieve satisfactory quality of printed products. This can be explained by the fact that on classic screen printing meshes are closed at the bottom by the substrate, which does not allow the ink to pass through the cell. In addition, a conventional squeegee made of elastic material (rubber, polyurethane) is deformed under the pressure of the press, reducing the ink pressure.

The obtained data allow us to conduct a qualitative analysis of the technological process of ink filling the meshes. The base for comparison of calculated values with experimental ones is also created.

V. Conclusion

For the first time, a model of the plates flow with circulation was developed. With its help, the pressure distribution in the ink was obtained during the movement of the dosing squeegee. The use of Poiseuille's law allows one to obtain the dependence of ink penetration into the meshes on the angle of inclination and velocity of movement of the dosing squeegee. So for 12 PA viscosity ink its penetration is 25...280 microns for the 75°...105° inclination angles of the dosing squeegee and its velocity of 2 cm/s...20 cm/s.

The reliability of the study is determined by the use of fundamental mathematics and hydromechanics. To state the applicability range of the developed model, it is necessary to conduct full-scale experiments, which determine the next stage of work.

References

[1] Jiajer Ho 2018 Great Britain Rear-surface line-contact optimization using screen-print techniques on crystalline solar cells for industrial applications *Mat. Sci. in Semiconductor Proc.* **83** 22 – 6

[2] Raminafshar C 2018 Great Britain Carbon based perovskite solar cells constructed by screen-printed Components *Electrochimica Acta* **276** 261 – 7

[3] Ashebir G 2016 Netherlands Fully screen printed LRC resonant circuit *Microelectronic Eng.* **162** 6 – 11

[4] Dae U K 2016 Great Britain Effects of oxidation on reliability of screen-printed silver circuits for radio frequency applications *Microelectronics Reliability* **63** 120 – 4

[5] Molinero-Abad B 2018 Netherlands Comparison of backing materials of screen printed electrochemical sensors for direct determination of the sub-nanomolar concentration of lead in seawater *Talanta* **182** 549 – 57

[6] Jadav J K 2018 USA Development of silver/carbon screen-printed electrode for rapid determination of vitamin C from fruit juices *LWT - Food Sci. and Technology* **88** 152 – 8

[7] Pellitero M A 2018 USA Antimony tin oxide (ATO) screen-printed electrodes and their application to spectroelectrochemistry *Electrochemistry Communications* **93** 123-7

[8] Rawlinson S 2018 USA Rapid determination of salicylic acid at screen printed electrodes *Microchem. J.* **137** 71 – 7

[9] González-Sánchez M I 2018 USA Highly activated screen-printed carbon electrodes by electrochemical treatment with hydrogen peroxide *Electrochem. Communications* **91** 36 – 40

[10] Pengjuan L and el. 2018 Netherlands Imprinted nanobead-based disposable screen-printed potentiometric sensor for highly sensitive detection of 2-naphthoic acid *Materials Letters* **225** 138 – 41

[11] Saxena S 2018 Voltammetric study of multiwalled carbon nanotube modified screen printed carbon electrode for the determination of a phytoconstituent wedelolactone *Sci. Direct Proc.* **5** 9167 – 72

[12] Litunov S N and Filatov D S Ustroistvo dlia trafaretnoi pechati [Device for screen printing]. Patent RF, no 85399, 2009.

[13] Loitsyansky L G 2003 *Fluid and gas mechanics* (Moscow: Drofa) p 188